Chemical vapour deposition of Si_3N_4 from a gas mixture of Si_2Cl_6, NH_3 and H_2

SEIJI MOTOJIMA, NORIYUKI IWAMORI
Department of Industrial Chemistry, Faculty of Engineering, Gifu University, Gifu 501-11, Japan

TATSUHIKO HATTORI
Research Laboratory, Toa-Gosei Chemical Industry Co. Ltd, 1-1 Funamicho, Minato-ku, Nagoya 455, Japan

Si_3N_4 layers were obtained on a quartz substrate from a gas mixture of Si_2Cl_6, NH_3 and H_2 under a reduced pressure in a temperature range of 800 to 1300° C. Amorphous Si_3N_4 layers that were dense and adherent to the substrate were obtained in a temperature range of 800 to 1100° C. On the other hand, α-Si_3N_4 layers were obtained at 1200° C and a source-gas ratio (N/Si) of 1.33 to 1.77. The lowest deposition temperature of amorphous Si_3N_4 was considered to be about 700° C. The microhardness of amorphous Si_3N_4 obtained in a temperature range of 800 to 1100° C was 2400 to 2600 kg mm^{-2} (load: 50 g), and that of α-Si_3N_4 obtained at 1200° C was 3400 kg mm^{-2}. Chlorine contents in the Si_3N_4 layer decreased with increasing deposition temperature and source-gas ratio (N/Si), and with decreasing total pressure.

1. Introduction

Silicon nitride has many excellent mechanical and chemical characteristics, such as high strength, high hardness, high thermal shock resistance (low thermal expansion and high thermal conductivity), good oxidation and corrosion resistivities, as well as good protective abilities against diffusion of O_2, H_2O, Na^+ and other diffusive species. Therefore, it is considered to be the most promising candidate for high-temperature engineering applications and for passivating the protective coatings of electronic devices.

Protective applications of Si_3N_4 coatings obtained by the CVD process, against wear, abrasion, erosion, oxidation and corrosion, have been extensively examined. For example, Si_3N_4-coated tools have been successfully applied for machining CuBe and aluminium alloys with a high silicon content, and can be used as punches or dies for forming copper and aluminium materials [1]; they are especially used at high speeds and rates where conventional tools cannot be used [2].

Si_3N_4 has been prepared from a number of silicon sources. SiH_4 has been exclusively used industrially to prepared Si_3N_4 layers for passivating protective applications to electronic devices [3–9]. Also, related compounds such as SiF_4 [10], SiF_2 [11] and SiH_3F [12] have recently been examined. Si_3N_4 coatings using a photo-CVD process sensitized by mercury vapour [13] or a magnetron sputtering process [14] have also been examined.

$SiCl_4$ has been used most frequently for the preparation of Si_3N_4 coatings which are intended for use in high-temperature mechanical applications. Hirai and co-workers [15–19] have reported the preparation of Si_3N_4 from a gas mixture of $SiCl_4$, NH_3 and H_2 under a reduced pressure of 5 to 300 torr in a temperature range of 1100 to 1500° C. Other silicon sources, such as $SiHCl_3$ [20], SiH_2Cl_2 [21–23], $SiBr_4$ [24] and $Si(CH_3)_4$ [25, 26] have also been examined. Morosanu [27] has reviewed the preparation, characterization and applications of Si_3N_4. Furthermore, Kingon *et al.* [28] have reviewed the preparation of Si_3N_4 by the CVD process, and summarized the literature. They have also calculated CVD phase diagrams using a computer program. The CVD phase diagram for the system $SiCl_4$–NH_3 reveals that Si_3N_4 may be deposited at 800° C, and the lowest deposition temperature decreases as the system pressure decreases. However the lowest deposition temperature of Si_3N_4 layers from the gas system $SiCl_4$–NH_3 actually obtained is 1000 to 1100° C.

Hexachlorodisilane (Si_2Cl_6) is now available commercially as a test sample reagent. Some of the physical and thermodynamical properties of Si_2Cl_6 are shown in Table I. This compound is more unstable, and has a higher activity than that of $SiCl_4$. Thus, using Si_2Cl_6 as a silicon source, it is expected to form Si_3N_4 deposits at lower temperatures than in the case of $SiCl_4$. We have reported on the deposition of SiC layers from a gas mixture of Si_2Cl_6, C_3H_8 and H_2 [29].

TABLE I Some properties of hexachlorodisilane (Si_2Cl_6)

Melting point	−1° C
Boiling point	144° C
Vapour pressure	$\log P = 5.98 - 911/(t + 145)$ (P; mm Hg, t; ° C)
Heat of evaporation	42 kJ mol^{-1}
Heat of formation	986.5 kJ mol^{-1}
Specific heat	$C_p = 42.15 + 1.03 \times 10^{-3}T - 8.46 \times 10^5 T^{-2}$ (T; K)

0022–2461/86 $03.00 + .12 © *1986 Chapman and Hall Ltd.*

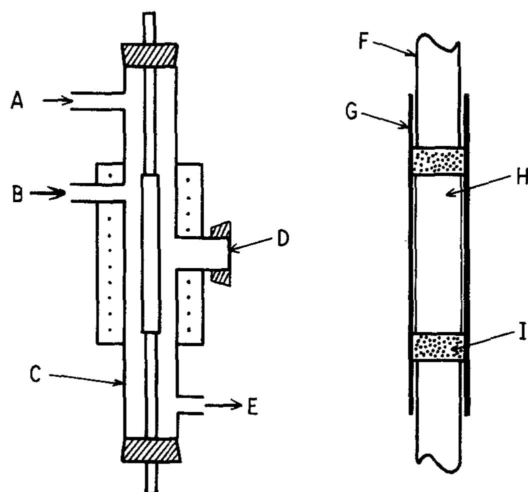

Figure 1 Experimental apparatus. (A) NH_3, H_2 and argon inlet, (B) Si_2Cl_6 and H_2 inlet, (C) reactor (quartz, 22 mm i.d. and 400 mm long), (D) observation window, (E) aspirator, (F) electrode, (G) substrate (quartz tube, 7 mm o.d. and 100 mm long), (H) SiC rod heater, (I) carbon powder.

In this work, we have obtained Si_3N_4 layers on a quartz substrate from a gas mixture of Si_2Cl_6, NH_3 and H_2 under a reduced pressure, and examined the growth conditions and some of the properties of the Si_3N_4 layers obtained.

2. Experimental procedure

Si_2Cl_6 (purity at least 99.5%) was obtained from Toa-Gosei Chemical Industrial Co., Japan. High-purity NH_3 gas (99.99%) obtained commercially was used without further purification. H_2 and argon gases were purified by passing through molecular sieves. The experimental apparatus used is shown schematically in Fig. 1. In the central part of the reaction tube (quartz, 22 mm internal diameter and 400 mm long), a tubular substrate (quartz, 7 mm outer diameter and 100 mm long) was located and heated dually from the outer nichrome element and an inner SiC rod heater. The temperature of the substrate was measured using an optical pyrometer from the observation window.

Elemental analysis of the Si_3N_4 deposits obtained was carried out using an energy-dispersive type of electron probe microanalyser (Akashi, EMAX-8000S). In this work, the gas flow rates of Si_2Cl_6, NH_3 and H_2 were fixed at 0.028, 0.1 and 1.0 ml sec^{-1}, respectively, unless otherwise described. Also, the total gas pressure was fixed at 25 torr unless otherwise described.

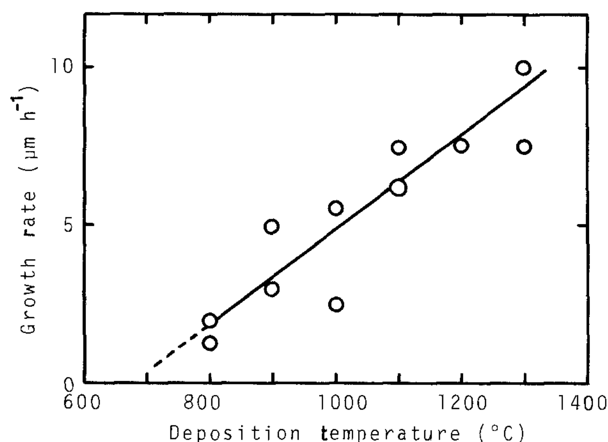

Figure 2 Effect of the deposition temperature on the growth rate of Si_3N_4 layers. Si_2Cl_6 flow rate: 0.028 ml sec^{-1}, NH_3 flow rate: 0.1 ml sec^{-1}, H_2 flow rate: 1.0 ml sec^{-1}, total gas pressure: 25 torr.

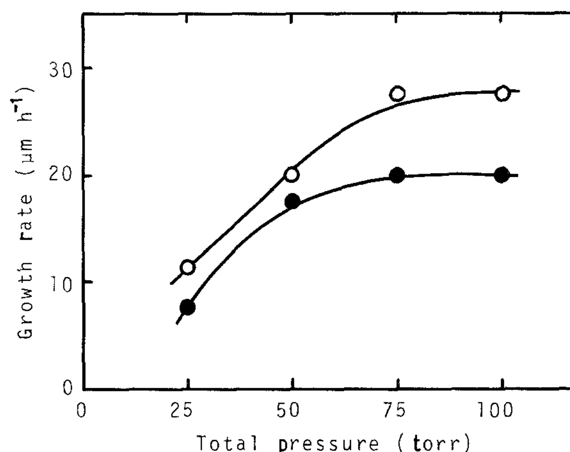

Figure 3 Effect of the total gas pressure on the growth rate of Si_3N_4 layers. Si_2Cl_6 flow rate: 0.028 ml sec^{-1}, NH_3 flow rate: 0.1 ml sec^{-1}, H_2 flow rate: 1.0 ml sec^{-1}. Deposition temperature: (●) 900° C, (○) 1000° C.

3. Results and discussion

3.1. Effect of deposition parameters on the deposition rate

The effect of deposition temperature on the growth rate of Si_3N_4 layers is shown in Fig. 2, in which the thickness of the Si_3N_4 layers was measured at the central part of the quartz substrate.

Apparent Si_3N_4 deposition was observed at 800° C and the growth rate increased linearly with increasing deposition temperature. In this work, deposition experiments could not be carried out at temperatures below 800° C, because of the limitations of the optical pyrometer. However, the lowest deposition temperature of Si_3N_4 is considered to be about 700° C. In the low-pressure CVD process, it is well known that the deposition rate and deposited phases are significantly affected by the total gas pressure, gas flow rates and ratios. The effect of the total gas pressure on the growth rate of the Si_3N_4 layers is shown in Fig. 3. The growth rate increased with increasing total gas

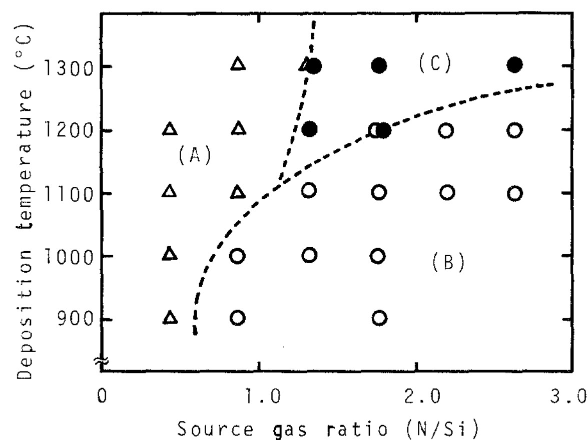

Figure 4 Effect of the source gas ratio (N/Si) and deposition temperature on the deposited phases. Si_2Cl_6 flow rate: 0.028 ml sec^{-1}, H_2 flow rate: 1.0 ml sec^{-1}, total gas pressure: 25 torr. (△) Silicon single phase or mixed phase of silicon and amorphous Si_3N_4 (Region A), (○) amorphous Si_3N_4 single phase (Region B), (●) α-Si_3N_4 phase (Region C).

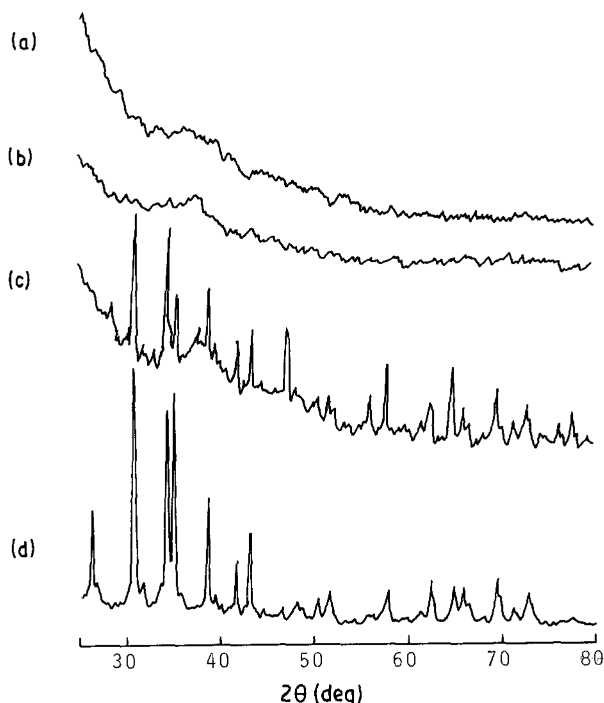

Figure 5 Representative X-ray diffraction patterns (Cu$K\alpha$ radiation). Si_2Cl_6 flow rate: 0.028 ml sec^{-1}, NH_3 flow rate 0.1 ml sec^{-1}, H_2 flow rate: 1.0 ml sec^{-1}, total gas pressure: 25 torr, deposition temperature: (a) 800° C, (b) 1100° C, (c) 1200° C. (d) Commercially obtained α-Si_3N_4 (99.99% purity).

pressure and attained a constant value at pressures above 75 torr, irrespective of the growth temperature. This increase of the growth rate is probably caused by the increase of the residence time in the reaction zone of reactant gases. A similar tendency has been observed by Hirai *et al.* [16] in the deposition of Si_3N_4 from a gas mixture of $SiCl_4$, NH_3 and H_2. At the deposition temperature of 1100° C, the growth rate increased with increasing source gas ratio of N/Si and attained a constant at the stoichiometric ratio of N/Si = 1.33. On the other hand, at 1200° C, maximum growth rate was attained at the stoichiometric ratio. The growth rate increased with increasing source gas ratio H/Cl, and the value obtained at the ratio H/Cl = 35 was three times higher than that obtained at H/Cl = 10.

3.2. Effect of deposition parameters on the phase and morphology of the deposits

The effect of the source gas ratio (N/Si) and deposition temperature on the phase of the deposits is shown in Fig. 4, in which the flow rate of Si_2Cl_6 was fixed at 0.028 ml sec^{-1} and that of NH_3 was varied. Phases were determined using X-ray diffraction, etching tests and the Vickers microhardness. Deposition of single-phase silicon or mixed phases of silicon and amorphous Si_3N_4 layers were observed at a lower source gas ratio (N/Si) than the stoichiometric ratio of Si_3N_4(N/Si = 1.33) (Region A in Fig. 4), irrespective of the deposition temperature. An amorphous Si_3N_4 phase was obtained at low deposition temperatures (Region B). On the other hand, above the stoichiometric source gas ratio (N/Si = 1.33) and above 1200° C, deposition of α-Si_3N_4 phase was confirmed by X-ray diffraction (Region C).

Representative X-ray diffraction patterns from the surfaces of the deposits are shown in Fig. 5, together with that of commercially obtained α-Si_3N_4 powder (99.99% purity). Appreciable α-Si_3N_4 peaks are observed for the deposits obtained at 1200° C. However, no apparent peaks were seen for deposits obtained below 1100° C, indicating an amorphous phase.

The appearance of the surfaces of the Si_3N_4 layers obtained at various deposition temperatures are shown in Fig. 6. Amorphous Si_3N_4 layers obtained in a temperature range of 800 to 1100° C are translucent in thin layers with good adherence to the substrate, and small pebbles or hillocks without any crystal facets are observed on the surfaces (Figs 6a and b). On the other hand, many crystal facets can be seen on the

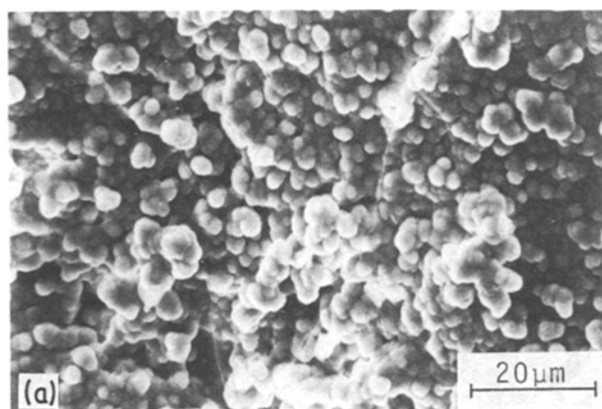

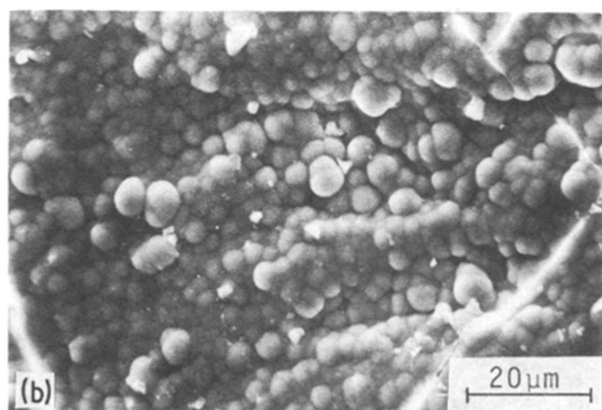

Figure 6 SEM photographs of the surfaces of Si_3N_4 layers. Si_2Cl_6 flow rate: 0.028 ml sec^{-1}, NH_3 flow rate: 0.1 ml sec^{-1}, H_2 flow rate: 1.0 ml sec^{-1}, total gas pressure: 25 torr, deposition temperature: (a) 800° C, (b) 1000° C, (c) 1200° C. (a) and (b) amorphous Si_3N_4, (c) α-Si_3N_4.

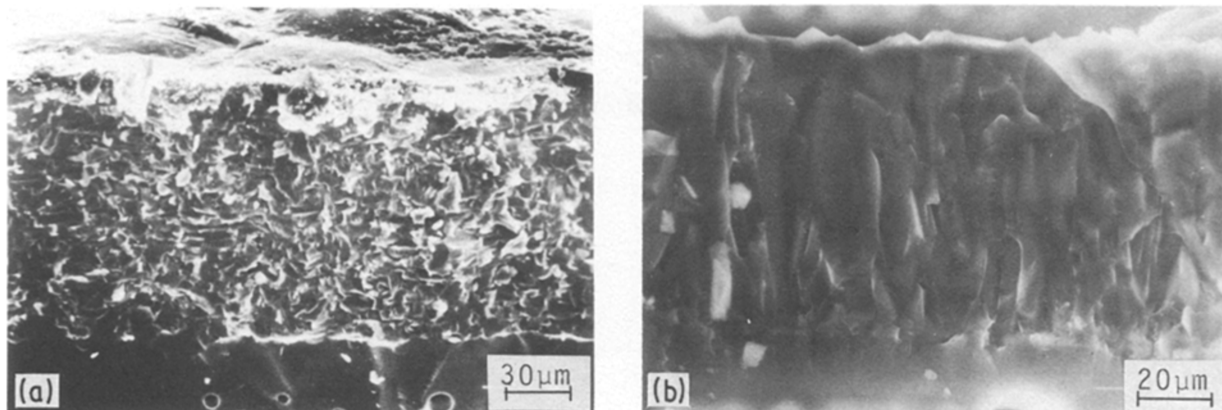

Figure 7 SEM photographs of the ruptured cross-sections of Si_3N_4 layers. Si_2Cl_6 flow rate: 0.028 ml sec^{-1}, NH_3 flow rate: 0.1 ml sec^{-1}, H_2 flow rate: 1.0 ml sec^{-1}, total gas pressure: 25 torr. (a) Amorphous Si_3N_4 deposited at 800° C, (b) α-Si_3N_4 deposited at 1300° C.

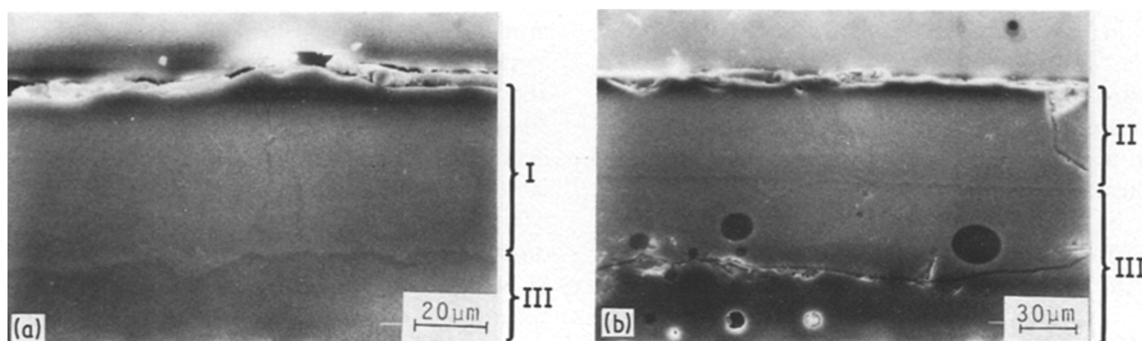

Figure 8 SEM photographs of the polished cross-sections of Si_3N_4 layers. Si_2Cl_6 flow rate: 0.028 ml sec^{-1}, NH_3 flow rate: 0.1 ml sec^{-1}, H_2 flow rate: 1.0 ml sec^{-1}. (a) Amorphous Si_3N_4 deposited at 800° C, (b) α-Si_3N_4 deposited at 1200° C; (I) amorphous Si_3N_4 layer, (II) α-Si_3N_4 layer, (III) quartz substrate.

surface of α-Si_3N_4 layers obtained at 1200° C (Fig. 6c). The appearance of the ruptured cross-sections of amorphous and α-Si_3N_4 layers are shown in Fig. 7. Small irregular crack patterns can be seen on the ruptured cross-section of an amorphous Si_3N_4 layer, while apparent columnar structures can be seen on that of α-Si_3N_4 layers. Amorphous Si_3N_4 layers were very dense and strongly adherent to the quartz substrate as can be seen in Fig. 8.

Various interesting surface morphologies of the Si_3N_4 obtained at 1200° C are shown in Fig. 9. At a low source gas ratio of N/Si (Region A in Fig. 4), pillar-like silicon co-deposition can be seen on an amorphous Si_3N_4 layer (Fig. 9a). On the other hand, α-Si_3N_4 globular polycrystals can be seen here and there on an amorphous Si_3N_4 layer obtained at

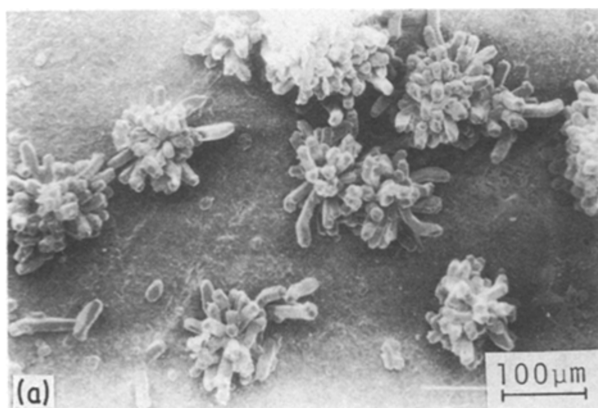

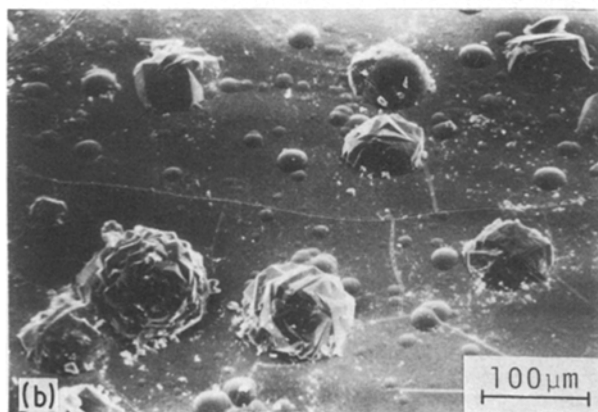

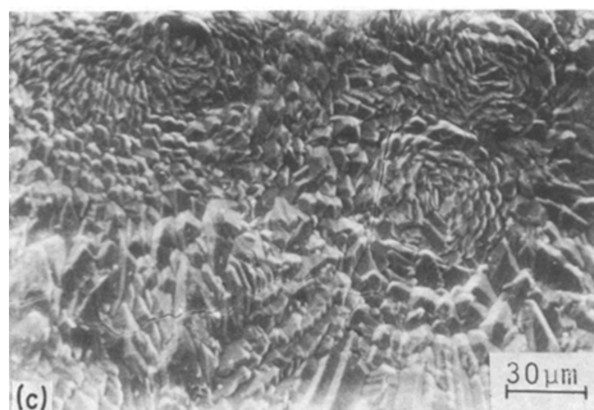

Figure 9 Peculiar surface morphologies. Deposition temperature: 1200° C. (a) Pillar-like silicon deposits formed on the amorphous Si_3N_4 layers in Region A of Fig. 4, (b) α-Si_3N_4 deposits formed on the amorphous Si_3N_4 layers at the boundary of Regions B and C in Fig. 4, (c) peculiar facet arrays of α-Si_3N_4 obtained in Region C of Fig. 4.

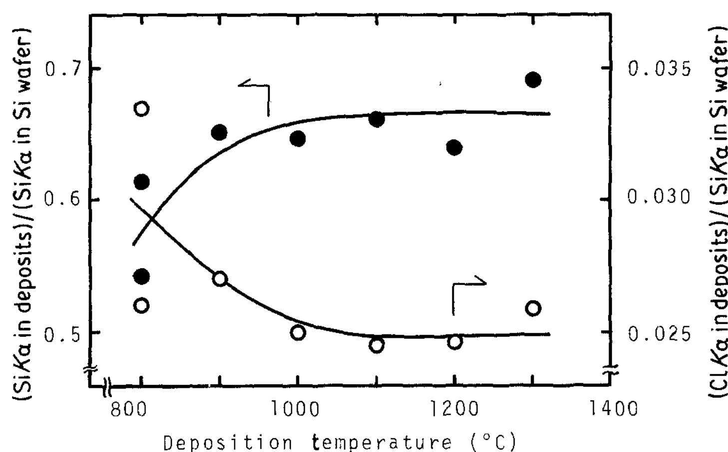

Figure 10 Effect of the deposition temperature on the silicon and chlorine contents in the Si_3N_4 layers. Si_2Cl_6 flow rate: 0.028 ml sec^{-1}, NH_3 flow rate: 0.1 ml sec^{-1}. (●) Silicon content, (○) chlorine content.

deposition conditions in the boundary of Regions B and C in Fig. 4 (Fig. 9b). Sometimes, circular crystal facet arrays were observed on the α-Si_3Ni_4 layers deposited in Region C of Fig. 4 (Fig. 9c). These facet arrays are probably formed by the development of crystal nuclei, as can be seen in Fig. 9b, formed here and there on the substrate.

α-Si_3N_4 layers obtained at 1200° C showed a slightly yellowish colour, and were tightly adherent to the substrate.

3.3. Effect of deposition parameters on the composition of the deposits

Silicon and chlorine contents in the Si_3N_4 deposits were estimated roughly by the ratio of the peak areas of Si$K\alpha$ (1.66 to 1.88 keV) and Cl$K\alpha$ (2.58 to 2.86 keV) in the deposits to that of Si$K\alpha$ (1.66 to 1.88 keV) of the silicon wafer, respectively. The effects of the deposition temperature on the silicon and chlorine contents in the deposits are shown in Fig. 10. The silicon content in the deposits increased with increasing deposition temperature and attained a constant value at temperatures above 900° C. On the other hand, the chlorine content decreased with increasing deposition temperature and attained a constant value of about 0.025. The low silicon content in the deposits obtained below 900° C is probably attributable to the inclusion of some amount of hydrogen and/or chlorine. The effects of the total gas pressure on the silicon and chlorine contents in the deposits are shown in Fig. 11, in relation to the deposition temperature. The silicon content decreased with increasing total gas pressure and attained a constant value at pressures above 50 torr. On the other hand, the chlorine content in the deposits obtained at 900° C increased rapidly with increasing total pressure and reached a high value of 0.04 at 75 torr. The effect of the source gas ratio (N/Si) on the silicon and chlorine contents in an amorphous Si_3N_4 obtained at 1100° C is shown in Fig. 12. The silicon content increased with increasing source gas ratio (N/Si) and attained a constant value at the stoichiometric ratio of N/Si = 1.33, while the chlorine content decreased gradually at ratios (N/Si) above 1.8. On the other hand, no appreciable effects of the source gas ratio (H/Cl) on the silicon and chlorine contents were observed at ratios above 18, as shown in Fig. 13.

In applications of Si_3N_4 layers to wear- or abrasion-resistant coatings, it may reasonably be considered that a high inclusion rate of chlorine in the coated layers causes severe deterioration of the resistance, as in the case of TiN-coated cutting inserts in which flank wear increased exponentially with increasing chlorine content [30]. Thus, it may be considered that more highly wear- or abrasion-resistant coating layers of Si_3N_4 are obtained at low total pressures below 50 torr, high deposition temperatures above 1000° C, and high source gas ratios of N/Si above 1.8.

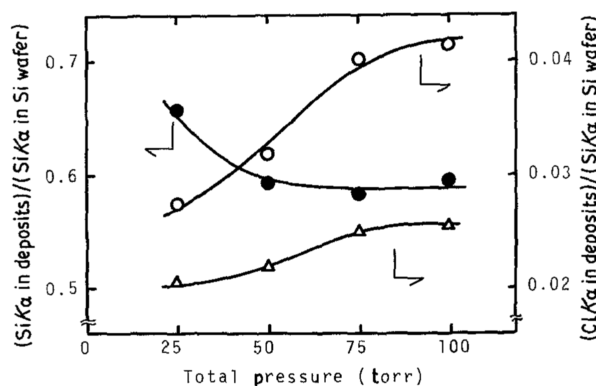

Figure 11 Effect of the total gas pressure on the silicon and chlorine contents in the Si_3N_4 layers. Si_2Cl_6 flow rate: 0.028 ml sec^{-1}, NH_3 flow rate: 0.1 ml sec^{-1}, H_2 flow rate: 1.0 ml sec^{-1}. (●) Silicon content of amorphous Si_3N_4 obtained at 900° C, (○) chlorine content of Si_3N_4 obtained at 900° C, (△) chlorine content of α-Si_3N_4 obtained at 1200° C.

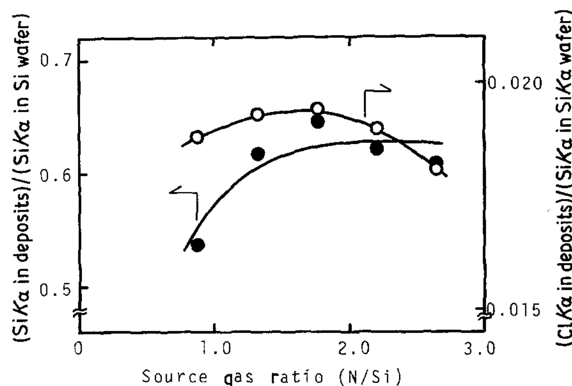

Figure 12 Effect of the source gas ratio (N/Si) on the silicon and chlorine contents in the Si_3N_4 layers. Si_3N_4 flow rate: 0.028 ml sec^{-1}, deposition temperature: 1100° C, total gas pressure: 25 torr. (●) Silicon content, (○) chlorine content.

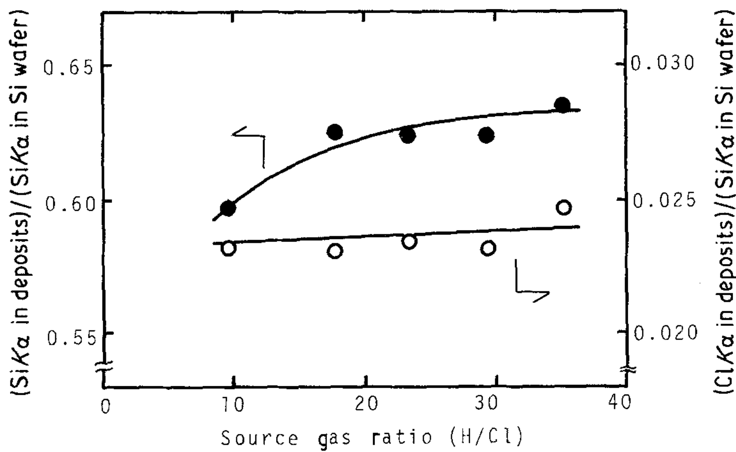

Figure 13 Effect of the source gas ratio (H/Cl) on the silicon and chlorine contents in the Si_3N_4 layers. Si_2Cl_6 flow rate: 0.028 ml sec^{-1}, NH_3 flow rate: 0.1 ml sec^{-1}, deposition temperature: 1100° C, total gas pressure: 25 torr. (●) Silicon content, (○) chlorine content.

3.4. Effect of deposition parameters on the Vickers microhardness

The Vickers microhardness of the Si_3N_4 layers was measured on polished cross-sections using a hardness tester (Akashi, MVK-1). The effect of the deposition temperature on the Vickers microhardness of Si_3N_4 layers is shown in Fig. 14. The hardness was measured at room temperature and an indentation load of 50 g. The hardness of the amorphous Si_3N_4 layers obtained at 800° C was about 2400 kg mm^{-2}, and it increased gradually with increasing deposition temperature, followed by a rapid increase at temperatures above 1000° C to the high value of 3400 kg mm^{-2} for the α-Si_3N_4 obtained at 1200° C. These values are considerably higher than that reported by Niihara and Hirai [31]. The effect of the total gas pressure on the Vickers microhardness of amorphous Si_3N_4 layers obtained at 900° C is shown in Fig. 15. The hardness decreased gradually with increasing total gas pressure, as in the case using $SiCl_4$ as a silicon source [31]. These results show that high hardness is obtained at deposition temperatures above 1000° C and total gas pressures below 50 torr.

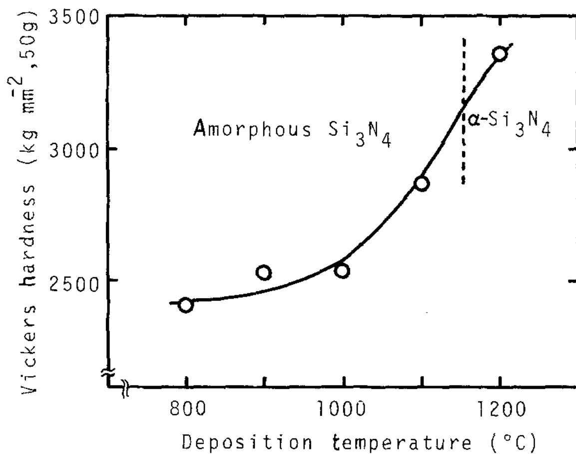

Figure 14 Effect of the deposition temperature on the Vickers microhardness. Si_2Cl_6 flow rate: 0.028 ml sec^{-1}, NH_3 flow rate: 0.1 ml sec^{-1}, H_2 flow rate: 1.0 ml sec^{-1}, total gas pressure: 25 torr. Indentation load: 50 g.

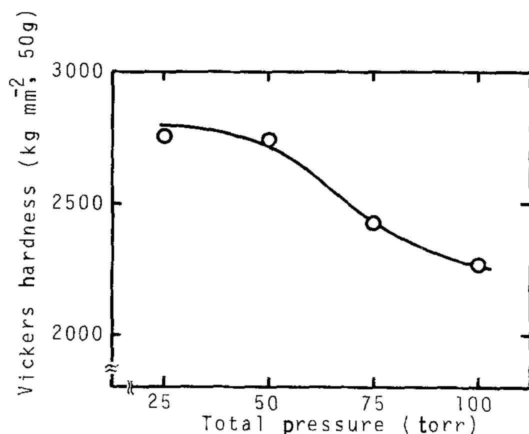

Figure 15 Effect of the total gas pressure on the Vickers microhardness of amorphous Si_3N_4 layers. Si_2Cl_6 flow rate: 0.028 ml sec^{-1}, NH_3 flow rate: 0.1 ml sec^{-1}, H_2 flow rate: 1.0 ml sec^{-1}, deposition temperature: 900° C.

References

1. W. HÄNNI and H. E. HINTERMANN, in Proceedings of 8th International Conference on CVD, Gouvieux, France, 1981 (The Electrochemical Society, Pennington, 1981) p. 597.
2. M. FUKUHARA, K. FUKAZAWA and A. FUKAWA, *Wear* **102** (1985) 195.
3. M. MAEDA and Y. ARITA, *J. Appl. Phys.* **53** (1982) 6852.
4. K. KATOH, M. YASUI and H. WATANABE, *Jpn J. Appl. Phys.* **22** (1983) L321.
5. C. BLAAUW, *J. Electrochem. Soc.* **131** (1984) 1114.
6. H. Y. KUMAGAI, in Proceedings of 9th International Conference on CVD, Cincinatti, Ohio, 1984 (The Electrochemical Society, Pennington, 1984) p. 189.
7. V. S. NGUYEN, *ibid.* p. 213.
8. Y. K. FANG, C. F. HUANG, C. Y. CHANG and R. H. LEE, *J. Electrochem. Soc.* **132** (1985) 1222.
9. K. ALLAERT, A. VAN CALSTER, H. LOOS and A. LEGUESNE, *ibid.* **132** (1985) 1763.
10. F. FUJITA, H. TOYOSHIMA, T. OHISHI and A. SAKAKI, *Jpn J. Appl. Phys.* **23** (1984) L144.
11. *Idem, ibid.* **23** (1984) L268.
12. A. MATSUDA, K. YAGI, T. KAGA and K. TANAKA, *ibid.* **23** (1984) L576.
13. K. HAMANO, Y. NUMAZAWA and K. YAMAZAKI, *ibid.* **23** (1984) 1209.
14. T. SERIHARA and A. OKAMOTO, *J. Electrochem. Soc.* **131** (1984) 2928.
15. K. NIIHARA and T. HIRAI, *J. Mater. Sci.* **11** (1976) 593.
16. T. HIRAI, K. NIIHARA and T. GOTO, *J. Jpn Inst. Met.* **41** (1977) 358.
17. *Idem, J. Mater. Sci.* **12** (1977) 631.
18. T. HIRAI and S. HAYASHI, in Proceedings of 8th International Conference on CVD, Gouvieux, France, 1981 (The Electrochemical Society, Pennington 1981) p. 790.
19. T. HIRAI, *Mater. Sci. Res.* **17** (1984) 329.
20. J. BÜHLER, E. FITZER and D. KEHR, in Proceedings of 6th International Conference on CVD, Atlanta, Georgia, 1977 (The Electrochemical Society, Princeton, 1977) p. 493.

21. C. E. MOROSANU and E. SEGAL, *Thin Solid Films* **88** (1982) 339.
22. *Idem, ibid.* **91** (1982) 251.
23. T. MAKINO, *J. Electrochem. Soc.* **130** (1983) 450.
24. J. A. ABOAF, *ibid.* **116** (1969) 1736.
25. J. F. LARTIGUE, M. DUCARROIR and B. ARMAS, in Proceedings of 9th International Conference on CVD, Cincinatti, Ohio, 1984 (The Electrochemical Society, Pennington, 1984) p. 561.
26. J. F. LARTIGUE and F. SIBIEUDE, *ibid.* p. 583. 9th International Conference on CVD, 1984, p. 583.
27. C. -E. MOROSANU, *Thin Solid Films* **65** (1980) 171.
28. A. I. KINGON, L. J. LUTZ and R. F. DAVIS, *J. Amer. Ceram. Soc.* **66** (1983) 551.
29. S. MOTOJIMA, N. IWAMORI, T. HATTORI and K. KUROSAWA, *J. Mater. Sci.* **21** (1986) 1363.
30. N. KIKUCHI, Y. OOSAWA and A. NISHIYAMA, in Proceedings of 9th International Conference on CVD, Cincinatti, Ohio, 1984 (The Electrochemical Society, Pennington, 1984) p. 728.
31. K. NIIHARA and T. HIRAI, *J. Mater. Sci.* **12** (1977) 1243.

Received 18 November 1985
and accepted 10 January 1986